The Molecular Origin of the Inhibition of Transducin Activation in Rhodopsin Lacking the 9-Methyl Group of the Retinal Chromophore: A UV−Vis and FTIR Spectroscopic Study†

Reiner Vogel,‡ Gui-Bao Fan,§ Mordechai Sheves,§ and Friedrich Siebert*,‡

Sektion Biophysik, Institut für Molekulare Medizin und Zellforschung, Albert-Ludwig-Universität Freiburg, Albertstrasse 23, D-79104 Freiburg, Germany, and Department of Organic Chemistry, Weizmann Institute of Science, Rehovot 76100, Israel

Received April 14, 2000; Revised Manuscript Received May 31, 2000

ABSTRACT: The formation of the active rhodopsin state metarhodopsin II (MII) is believed to be partially governed by specific steric constraints imposed onto the protein by the 9-methyl group of the retinal chromophore. We studied the properties of the synthetic pigment 9-demethyl rhodopsin (9dm-Rho), consisting of the rhodopsin apoprotein regenerated with synthetic retinal lacking the 9-methyl group, by UV−vis and Fourier transform infrared difference spectroscopy. Low activation rates of the visual G-protein transducin by the modified pigment reported in previous studies are shown to not be caused by the reduced activity of its MII state, but to be due to a dramatic equilibrium shift from MII to its immediate precursor, MI. The MII state of 9dm-Rho displays only a partial deprotonation of the retinal Schiff base, leading to the formation of two MII subspecies absorbing at 380 and 470 nm, both of which seem to be involved in transducin activation. The rate of MII formation is slowed by 2 orders of magnitude compared to rhodopsin. The dark state and the MI state of 9dm-Rho are distinctly different from their respective states in the native pigment, pointing to a more relaxed fit of the retinal chromophore in its binding pocket. The shifted equilibrium between MI and MII is therefore discussed in terms of an increased entropy of the 9dm-Rho MI state due to changed steric interactions.

Light activation of rhodopsin is the first step in the reaction cascade of visual perception. Rhodopsin is an integral membrane protein with seven membrane spanning helices interconnected by intra- and extracellular loops and belongs to the large superfamily of G-protein-coupled receptors (*1*). Bovine rhodopsin (Rho)[1] from rod outer segments (ROS) of cattle retinae is the best understood member of this family, which is in part due to its availability in larger amounts for biophysical studies, and may therefore serve as a model for other G-protein-coupled receptors. Rhodopsin consists of the apoprotein opsin and its chromophore 11-*cis*-retinal, covalently linked to Lys^{296} on helix 7 of the opsin by a protonated Schiff base bond. The holoprotein has in the dark state an absorption maximum at 500 nm. Upon absorption of a single photon, the chromophore isomerizes within 200 fs (*2*) to the all-trans geometry, and the protein relaxes via several intermediates to metarhodopsin I (MI, λ_{max} 478 nm), which is formed after about 100 μs (*3*). MI forms in milliseconds a temperature- and pH-dependent equilibrium with metarhodopsin II (MII, λ_{max} 380 nm) (*4*). MII is the active conformation of the protein, which in turn catalyzes nucleotide exchange in the visual G-protein transducin and starts the reaction cascade of visual perception (*5*, *6*).

MI is the energetically lowest state in the relaxation process following photon absorption (*7*, *8*). The transition to MII is therefore entropy-driven and characterized by a major rearrangement of the protein, particularly by a movement of helix 3 relative to helices 6 and 7, which was detected by site-directed spin labeling (*9*), introduction of metal ion binding sites (*10*), and disulfide cross-linking experiments (*11*). This intramolecular rearrangement is accompanied by a transfer of the Schiff base proton to the counterion Glu^{113} (*12*) and an at least transient protonation of Glu^{134} at the cytoplasmic interface of helix 3 (*13*).

Recent studies on site-directed mutants suggested that the concerted helix rearrangement and thus activation of the receptor is linked to specific interactions between Gly^{121} on helix 3, Phe^{261} on helix 6, and the 9-methyl group of the retinal (*14*). A refined structural model of the retinal binding pocket was developed, which takes into account NMR constraints of the environment of the chromophore (*15*). According to this model, Gly^{121} and Phe^{261} are in juxtaposition across the chromophore binding pocket and mediate specific retinal−protein contacts, which in part define this

† This work was supported by grants from the Deutsche Forschungsgemeinschaft to R.V. (Grant VO 811/1-1) and to F.S. (Grant SI 278/16-2,3), by the Fonds der Chemischen Industrie (to F.S.), by the Dr. Cohen MINERVA Center for Biomembrane Research (to M.S.), and by the U.S.−Israel Binational Science Foundation (to M.S.).

* Corresponding author. Tel.: (49) 761 203 5396, Fax: (49) 761 203 5399, e-mail: frisi@uni-freiburg.de.

‡ Albert-Ludwig-Universität Freiburg.

§ Weizmann Institute of Science.

[1] Abbreviations: Rho, rhodopsin; Iso, isorhodopsin; ROS, rod outer segment(s); 9dm, 9-demethyl; MI, metarhodopsin I; MII, metarhodopsin II; PP, photoproduct; *A*, absorbance; FTIR, Fourier transform infrared; HOOP, hydrogen-out-of-plane vibration; DM, dodecyl maltoside; ConA, concanavalin A; MES, 2-morpholinoethanesulfonic acid; BTP, Bis-Tris-propane.

10.1021/bi000852b CCC: $19.00
Published on Web 07/06/2000

binding pocket (*16*). The 9-methyl group in particular is tightly held in position between these two residues. Other structural models of rhodopsin (*17, 18*) position Phe^{261} near the β-ionone ring, but further away from both the 9-methyl group and Gly^{121}.

Upon light absorption and subsequent isomerization of the retinal to the all-trans geometry, the chromophore is in a twisted conformation in the early intermediate bathorhodopsin of the reaction cascade, as deduced from resonance Raman (*19*) and infrared investigations (*20*), and relaxes progressively in the subsequent low-temperature intermediates BSI, lumirhodopsin, and MI. In MI, the protein is tightly packed around the chromophore in an energetically minimized conformation, albeit a conformation with also a low entropy (*3, 8*). The strain on the chromophore is considerably weaker, yet not fully released as deduced from the intensity of the hydrogen-out-of-plane (HOOP) modes in resonance Raman spectra (*21*) and FTIR spectra (*22*) derived from Rho MI. Only in the entropically higher MII state with its less tightly packed protein conformation (*4*), the chromophore is presumably in a relaxed all-trans geometry (*21*).

This local steric interaction between the retinal 9-methyl group and the protein conformation is termed the "steric trigger" in rhodopsin activation (*15*). Experimental evidence for this proposal is derived from site-directed mutant opsins that have Gly^{121} replaced by amino acids with bulkier side chains, this leading to a correspondingly decreased uptake of 11-*cis*-retinal into the binding pocket (*23*). Moreover, the inverse agonist activity of 11-*cis*-retinal is reversed to a partial agonist activity with increasing volume of the side chain at position 121 as assayed by transducin activation of the respective dark pigment (*24*). This reversion could be inhibited by a specific second site replacement of Phe^{261} on helix 6 by a smaller residuum. In analogy, replacing the methyl group at C_9 of the retinal by larger ethyl or propyl groups led to a correspondingly increased dark and decreased light activity as well as an increased instability of the resulting pigment, presumably due to steric incompatibility (*14*).

This raises the question on the characteristics of a pigment without the functional 9-methyl group. Such a pigment was described first by Blatz (*25*) and Kropf (*26*), who noted the blue shifted λ_{max} of wild-type opsin regenerated with either 11-cis or 9-cis 9-demethyl retinal (9dm-retinal). The pigment resulting from regeneration with 11-cis 9dm-retinal (9dm-Rho) was investigated by an extensive FTIR and biochemical study (*22*). It was shown, that 9dm-Rho forms a red-shifted photoproduct (PP_{470}) with a protonated Schiff base linkage both at 80 K and at room temperature and neutral pH. The appearance of a red-shifted photoproduct was also confirmed by a kinetic study covering the time range from 20 ns to 1 μs at room temperature (*27*). Infrared difference spectra indicated a normal MII conformation of the photoproduct, yet with a protonated retinal Schiff base as deduced from the unusual position of the ethylene stretch mode of the chromophore. Despite this otherwise apparently normal MII state, as judged by infrared spectroscopy, transducin activation assays gave dramatically low values for G-protein activation by 9dm-Rho. A second, more detailed study on transducin activation (*28*) reported a higher activity of up to 43% in dependence of temperature in comparison to Rho. Although these studies clearly demonstrated the importance of the 9-methyl group for rhodopsin activation, the properties of the photoproduct of 9dm-Rho causing the reduced activation have not been characterized. Finally, 9dm-Rho, as assayed in regenerated salamander rod cells, showed a reduced quantal response, but a prolonged excitation of the photoreceptor due to reduced light-dependent phosphorylation of the receptor protein (*29, 30*)

In this paper we report on a changed MI/MII equilibrium of 9dm-Rho, that is extremely shifted to the MI side. MII is formed only under very favoring conditions, as low pH, high temperature and a fluid environment as present in a detergent micelle. In contrast to Rho, the transition from MI to MII is not strictly coupled to a deprotonation of the Schiff base and a concomitant shift of λ_{max} to the near UV. Instead we will report on a MII state with an only partially deprotonated retinal Schiff base resulting in two spectrally different MII forms, MII_{380} and MII_{470}, absorbing at 380 and 470 nm, respectively. The latter species is spectrally almost degenerate with the MI state, which has a similar λ_{max} with an only slightly smaller bandwidth. Both MI and MII_{470} form the red-shifted photoproduct PP_{470} as defined by visible spectroscopy. As λ_{max} of this visible photoproduct is very close to the absorbance maximum of the dark state, there is considerable photoregeneration of the dark state upon illumination, and consequently only a limited photoproduct yield is obtained. Finally, we will discuss published transducin activation results (*22, 28*) and show that they are in agreement with a fully active MII state of 9dm-Rho, taking the pigment's particular properties into account. The reported limited G protein activation of 9dm-Rho only reflects the shifted MI/MII equilibrium and the limited photoproduct yield of the pigment due to photoregeneration.

MATERIALS AND METHODS

Preparation of Rhodopsin. Rhodopsin (Rho) in washed rod outer segment disk membranes was isolated from retinae prepared from cattle eyes obtained from a local slaughterhouse essentially as described previously (*31*). For purification in detergent (*32*), disk membranes were solubilized in dodecyl maltoside (DM, Anatrace, OH) and loaded on a concanavalin A (Con A) Sepharose column (Pharmacia Biotech, Sweden). After washing with dodecyl maltoside buffer, purified Rho was eluted with methyl-α-D-mannopyranoside and dialyzed against 0.02% DM in distilled water. Both Rho in membranes and in detergent were stored at −20 °C. All manipulations involving Rho or 9dm-Rho were performed under dim red light.

Synthesis of 9-Demethyl Retinal. The synthesis of 11-cis and 9-cis 9dm-retinal was carried out according to methods described previously (*25, 33*).

Preparation of 9dm-Rho. 9dm-Rho in washed disk membranes was prepared from Rho by removal of the covalently bound retinal chromophore and subsequent regeneration of the opsin with the synthetic 11-cis 9dm-retinal. In detail, Rho in disk membranes was bleached thoroughly by white light at room temperature in the presence of 10 mM hydroxylamine in 100 mM phosphate buffer, pH 7.0. Hydroxylamine was removed by washing the disk membranes at 4 °C and 150000*g* twice with 10 mM and once with 1 mM phosphate buffer, pH 5.5. The membrane suspension was mixed rapidly with 11-cis 9dm-retinal (0.5−1-fold molar excess) dissolved

in ethanol (final concentration <1%). The suspension was kept for 2 h at room temperature, and the regeneration was followed spectrophotometrically. The regenerated membranes were washed again with distilled water and stored at −20 °C.

9dm-Isorhodopsin (9dm-Iso) was prepared similarly with 9-cis 9dm-retinal.

9dm-Rho in detergent was prepared by purification of the regenerated disk membranes on ConA−Sepharose in DM similar as described above for Rho. To remove excess retinal and retinal oxime completely, the pigment was thoroughly washed overnight on the sepharose column with approximately 100 mL of DM buffer.

UV−Visible Spectroscopy. UV−visible absorption spectroscopy was performed on a Perkin-Elmer Lambda 17 UV−Vis Spectrophotometer equipped with a thermostated cuvette holder. Spectra from pigment solutions in 0.1% DM were measured in 100 μL micro quartz cuvettes with 10 mm path length. The spectra were background and offset corrected. As buffers we used generally phosphate buffer and in some experiments 2-morpholinoethanesulfonic acid (MES) and bis-tris propane buffer (BTP), making a pH range from pH 3.5 to 10.0 accessible. The buffer concentration was 100 mM throughout, unless stated otherwise. Sandwich or film samples for UV−visible absorption spectroscopy were identical to those for infrared spectroscopy described below. For light-induced difference spectra, the samples were illuminated for 60 s by a 150 W slide projector through a GG475 cutoff filter (Schott, Germany) and a fiber optic. Flash photolysis was performed in the UV−vis spectrometer on pigment solutions by an external flash fitted to a fiber optic.

Quantification of Photoconversion and Total MII and MI Content by UV−Vis Spectroscopy. For a quantification of photoconversion, solutions of pigment in detergent and 100 mM phosphate buffer were illuminated for 1 min, and photoproduct spectra were recorded. Then 20 mM hydroxylamine (stock 1 M in 1 M NaOH) was added to the samples, which were subsequently warmed to 24 °C to allow photoproducts to react with hydroxylamine. After completion of the reaction (∼30 min), the amount of unreacted dark pigment was determined. The unreacted dark pigment was stable against further incubation at 30 °C for at least 2 h. Upon subsequent illumination with white light for 5 min, the amount of total pigment could be determined.

For a quantification of the total MII content from the 380 nm photoproduct subspecies MII_{380}, we recorded spectra as described above under conditions where the photoproduct consists entirely of MII (=MII_{380} + MII_{470}, recorded at 10 °C and pH 4.5; see Results). We determined the absorbance change at 380 nm, ΔA_{380}, between photoproduct and dark spectrum (Figure 3B: spectrum 2 − spectrum 1), ΔA_{470} between the photoproduct and the hydroxylamine-treated state (spectrum 2 − spectrum 3), the absorbance at 464 nm, $A_{464\ dark}$, of the dark state, and $A_{464\ HA}$ of the hydroxylamine-treated state (spectrum 3). Taking the sum of the absorbance changes of the two MII subspecies $\Delta A_{MII} = \Delta A_{380} + \Delta A_{470}$ as an approximate measure for the MII photoproduct absorbance and $\Delta A_{dark} = A_{464\ dark} - A_{464\ HA}$ as a measure for the equivalent dark absorbance, we get $\Delta A_{MII}/\Delta A_{dark} = 1.05 \pm 0.01$ (SD), as well as $\Delta A_{380}/\Delta A_{MII} = 0.36 \pm 0.01$ (SD, $n = 5$) under these conditions. From these relations, we calculated the total MII content from ΔA_{380} of light-induced difference spectra obtained also under other conditions by the equation: $[MII] = (\Delta A_{380}/A_{464\ dark}) \times 2.64$ in units of the total pigment content of the sample. This extrapolation depends on a constant value of the ratio $\Delta A_{380}/\Delta A_{MII}$ (see next paragraph).

For quantification of the MI content in the photostationary state, we used the following approximation for the absorbance at 466 nm after illumination: $A_{466\ light} \approx A_{470\ MI} + A_{470\ MII} + A_{464\ regen.\ dark}$, the last term being due to photoregeneration of the dark state. With the determined relative absorption coefficients of the three states [dark and regenerated dark, 1; MI, 1.41; MII, 1.05 (assuming that both MII species have similar absorption coefficients)], we can rewrite this equation in terms of concentrations. With the conservation equation [MI] + [MII] + [regen. dark] = 1 (all concentrations in units of the total pigment concentration of the sample) and [MII] as determined above, we get after some basic calculation the approximation $[MI] \approx [(A_{466\ light} + \Delta A_{380} \times 0.866)/A_{464\ dark} - 1]/0.41$. This value represents only an estimate and depends as in the case of [MII] on a constant value for the MII_{380}/MII_{470} ratio. The validity of this assumption was tested by two methods: (a) The MII content was determined from sandwich samples in detergent by UV−vis spectroscopy employing the described method and found consistent with the MII content derived by FTIR spectroscopy on identical samples for temperatures up to 24 °C and pH ≥4.5. (b) The UV−vis method derives values for [MI] and [MII] from the three experimentally accessible values ΔA_{380}, $A_{464\ dark}$, and $A_{466\ light}$. By the hydroxylamine method, however, we can experimentally obtain a fourth value, $A_{464\ HA}$, and thus calculate the amount of photoregenerated dark state, or, equivalently, the amount of photoproduct [PP]. Cross-checking the calculated values for [MI] and [MII] (both based on a constant value of the MII_{380}/MII_{470} ratio) with the conservation equation [PP] = [MI] + [MII] gave consistent results. It must be noted that the first method is quite accurate, but cannot be applied to solutions, while the second analysis largely employs the difference between the extinction coefficients of MI and MII.

Quantification of the Schiff Base Hydrolysis Rates of Rhodopsin. Schiff base hydrolysis was assayed by acid denaturation of the MII photoproduct of purified Rho in DM at specified times after bleaching. Samples were bleached at 24 °C for 1 min through a GG495 filter. The UV−vis spectra of the denatured samples were fitted to two Gaussian peaks centered at 380 and 440 nm. The ratio $I_{440}/(I_{380} + I_{440})$, where I is the respective peak intensity, was taken as a measure for the amount of pigment with a still intact retinal Schiff base linkage. Replacing the peak intensities by the respective peak integrals gave similar results.

FTIR Spectroscopy. FTIR spectroscopy was performed with a Bruker IFS 28 FTIR spectrometer, equipped with a liquid nitrogen cooled Hg−Cd−Te detector and a dry air purged measuring chamber with a sample holder thermostated by a circulating water bath. Difference spectra were calculated from each 512 to 2048 scans recorded at a 4 cm^{-1} resolution before and after illumination. Illumination conditions were similar as described for UV−visible spectroscopy.

Samples for infrared transmission spectroscopy were sandwich samples. Sandwich samples were prepared on specially designed CaF_2 windows by drying approximately

0.5 nmol of pigment on a round spot of 7 mm diameter, separated from the 4 μm higher rim of the window by a 1 mm wide depression. The dried sample was hydrated by 0.5 μL of 100 mM phosphate buffer (at pH 8.5 borate substituted for phosphate) and sealed by placing a second, plane window onto the first window with its higher rim serving as a spacer. The buffer capacity of the phosphate buffered samples was found to be sufficient even at pH 4.5, as assessed by comparison of difference spectra derived from membrane samples with 100 mM phosphate, 100 mM MES, or 500 mM MES buffer.

In a few cases we used re-hydrated film samples. These samples were prepared by drying approximately 1 nmol of pigment with 5 μL of 100 mM phosphate buffer of the desired pH under nitrogen on a CaF_2 window. The samples were re-hydrated and sealed with a second CaF_2 window separated by a 5 mm spacer. The resulting water content of film samples was determined by the water absorbance bands at 3500, 2200, and 1650 cm^{-1}.

Determination of MII Content from FTIR Difference Spectra. The conformational state of the samples was determined by evaluation of characteristic MII difference bands in the carboxyl range. All spectra were first normalized by their +1272/−1235 cm^{-1} difference band, which is insensitive to the MI/MII transition. For detergent samples, we determined then $\Delta = \Delta A_{1755} - \Delta A_{1769}$ from essentially pure MI (Δ_{MI}) and MII (Δ_{MII}) difference spectra and assigned them a MII content of 0 and 1, respectively. By determining the corresponding Δ values from all other samples, we could determine their MII content by the linear interpolation $[MII] = (\Delta - \Delta_{MI})/(\Delta_{MII} - \Delta_{MI})$ in units of the total photoproduct concentration. We repeated this procedure with $\Delta = \Delta A_{1713} - \Delta A_{1726}$ and averaged over the two values for the MII content. Reference spectra were recorded at pH 7.5 and 1 °C for MI and at pH 4.5 and 10 °C for MII (see Results). The same procedure was used for membrane samples, yet with differing wavenumbers ($\Delta A_{1750} - \Delta A_{1767}$ and $\Delta A_{1710} - \Delta A_{1695}$), that proved to be more appropriate due to the differing band pattern in the carboxyl range for membrane and detergent samples. Application of the wavenumbers set used for detergent samples to membrane spectra led to inconsistent results and vice versa. The pure spectra for pigment in membrane were derived from sandwich samples at pH 7.5 and 1 °C for MI. As we observed no pure MII state in sandwich samples, we used for the MII reference spectra in membrane re-hydrated film samples at pH 4.5 and −3 °C, supplemented with additional NaCl to increase the ionic strength of the samples. Under conditions of extreme ionic strength, MII formation in 9dm-Rho is facilitated (Vogel, R., and Siebert, F., unpublished results), and we were thus able to obtain essentially pure MII difference spectra from membrane samples. We chose difference bands in the range of the C=O stretch mode of protonated carboxyl groups, as these are an indicator of the protein conformation and are insensitive to changes concerning the chromophore only. The amide I range is generally unreliable due to distortions by the strong background absorption of the amide I mode and the high water content of the samples. Difference bands in the amide II range, including the ethylenic mode of the chromophore, and chromophore bands in the fingerprint range, e.g. the difference bands at 1204 and 1148 cm^{-1}, may also serve as marker bands, however particularly the 1204 cm^{-1} band is influenced by changes in the MII_{380}/MII_{470} equilibrium and gives therefore inconsistent results at very low pH, where the Schiff base can be titrated (see Results and Figure 2b,c). We estimate the systematic error inherent in this method to be around 10% (absolute).

RESULTS

The Recombinant 9dm-Rho Dark Pigment. Opsin in membranes regenerated well with the retinal analogue 11-cis 9dm-retinal and the regeneration was completed within 2 h at room temperature. The purified protein has a visible absorption peak at λ_{max} 464 nm and a spectral ratio A_{280}/A_{464} of 2.7 in agreement with previous investigations (*22*, *25*, *26*, *28*). Bleaching of purified 9dm-Rho and Rho in the presence of 10 mM hydroxylamine at pH 7 yields opsin and the respective retinal oximes. Under the assumption that the two oximes have similar absorption coefficients, we can calculate from the absorbance of the oximes at 357 and 364 nm, respectively, a spectral ratio for the dark states $\epsilon_{9dm-Rho}/\epsilon_{Rho} = 0.90 \pm 0.03$ (mean ± SD). With the absorption coefficient for Rho $\epsilon_{500} = 42.7 \times 10^3$ cm^{-1} M^{-1}, the corresponding value for 9dm-Rho is $\epsilon_{464} = (38 \pm 1) \times 10^3$ cm^{-1} M^{-1}. The dark pigment purified in DM is stable against 20 mM hydroxylamine (no detectable formation of oxime within 1 h at 24 °C) and toward pH values ranging from 3.5 to 9.5 at 24 °C. Acid denaturation of the dark pigment yields the protonated Schiff base with an absorption peak at 432 nm compared to 440 nm for Rho, corresponding to the difference between the λ_{max} of the two free retinals (372 and 379 nm for 11-cis 9dm-retinal and 11-cis retinal, respectively).

The 9dm-Rho Photoproducts and the MI/MII Equilibrium. The 9dm-Rho photoproducts were examined both by UV−vis and FTIR spectroscopy. UV−vis spectroscopy was performed with solutions of purified pigment in 0.1% DM and in 100 mM phosphate buffer unless stated otherwise. Samples with unpurified pigment in membranes had the major disadvantage of considerable light scattering and residual absorbance of retinal oxime and unreacted 9dm-retinal from the regeneration procedure (Figure 1L,M). For FTIR spectroscopy, we tried to match the conditions of the UV−vis samples as far as possible and used sandwich samples with defined water content, ionic strength, and pH.

At 1 °C, 9dm-Rho forms at neutral pH, as described before (*22*, *28*), a red-shifted visible photoproduct (PP_{470}) with a protonated Schiff base (Figure 1C). At more acidic pH, the formation of an additional blue-shifted photoproduct is observed (Figure 1B) with a λ_{max} of 380 nm, as derived from difference spectra. This photoproduct PP_{380} exists in a rapid, pH-dependent equilibrium with PP_{470}. Interestingly, the PP_{380} yield in 100 mM phosphate buffer is maximal at pH 4.5 and decreases at more acidic pH (Figure 1A), indicating a re-protonation of the retinal Schiff base at low pH. The 380 nm photoproduct increases, when increasing the temperature to 10 °C (Figure 1D), but does not further increase at 24 °C (Figure 1G, spectrum 1′).

Infrared spectroscopy on solubilized 9dm-Rho under corresponding conditions reveals two photoproducts with distinct infrared spectra. At 10 °C and at pH 4.5 (Figure 2 a), the infrared difference spectrum of 9dm-Rho is with few exceptions identical to the respective MII difference spectrum

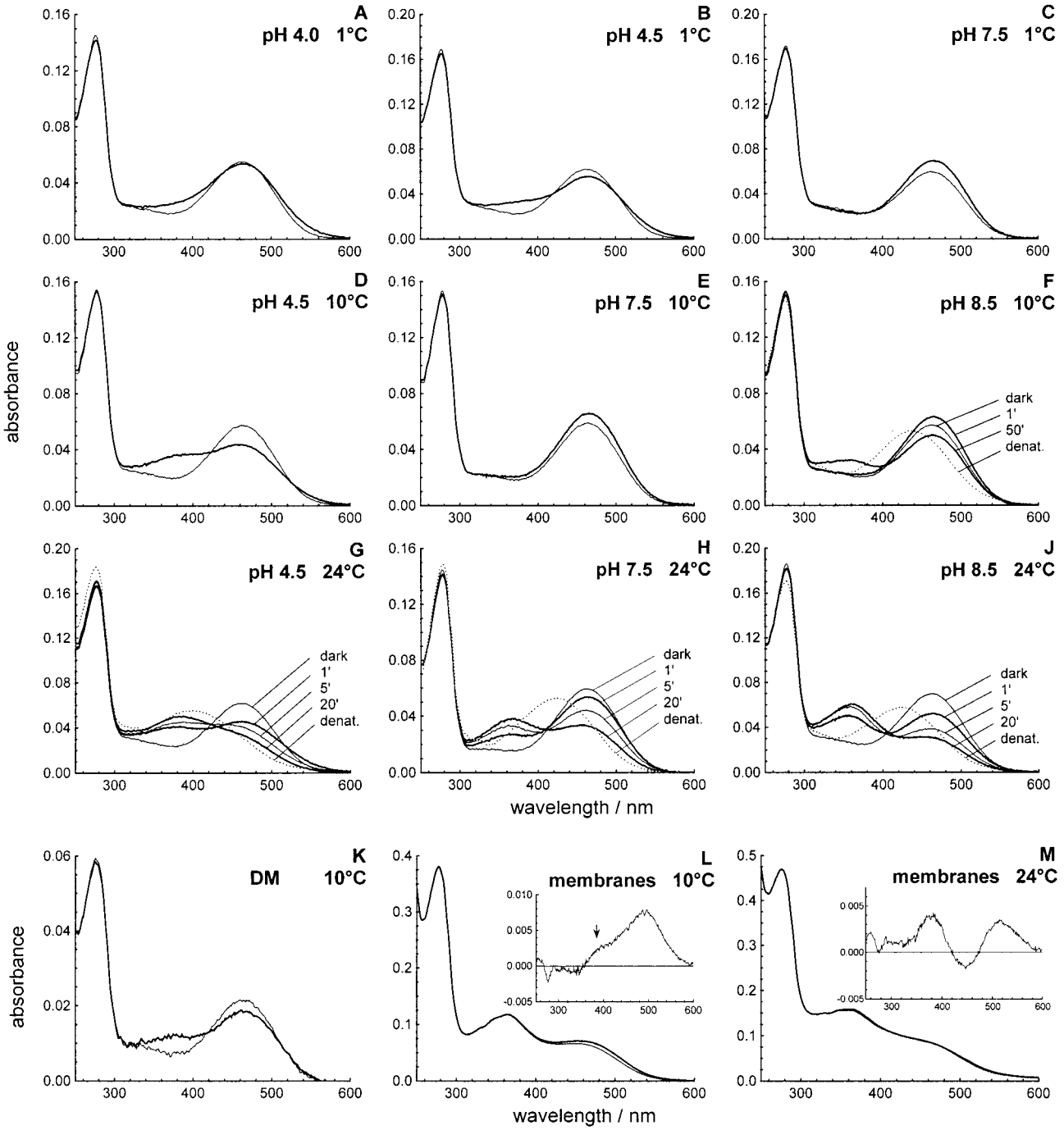

FIGURE 1: UV−vis spectra of 9dm-Rho. (A−J) Spectra of pigment in detergent in solution in 10 mM BTP buffer (F and J) or 100 mM phosphate buffer (all other spectra). Spectra were recorded of the dark state (thin line) and after a 1 min illumination (boldface line). When indicated, additional spectra were recorded at the specified time after illumination. At the end of some experiments, Schiff base hydrolysis was assayed by acid denaturation (addition of HCl) of the sample. (K−M) Spectra of pigment in sandwich samples (identical to those used for infrared spectroscopy) in detergent (K) and in membranes at two different temperatures (L and M) and pH 4.5. The insets in L and M show the light-induced difference spectra (photoproduct minus dark state).

of solubilized Rho under same conditions [cf. the corresponding Rho MII difference spectrum in membrane in Figure 5, that shows only minor differences to the respective spectrum in detergent, as already shown previously (*34*)]. This situation changes at lower temperatures (1 °C): While Rho forms at this temperature still a pure MII photoproduct (data not shown), in the 9dm-Rho spectrum there are contributions of a different photoproduct (Figure 2c). This photoproduct's difference spectrum can be obtained in its essentially pure form when increasing the pH to 7.5 (Figure 2d). It bears some resemblance to a Rho MI spectrum, the differences being, however, much more pronounced as compared to the differences between the MII spectra. Nevertheless, we will refer to both 9dm-Rho photoproducts described here in analogy to Rho as the respective 9dm-Rho MI and MII states, keeping in mind that there are distinct differences to the Rho MI and MII states.

With this information, we can correlate the photoproduct species PP_{380} and PP_{470}, that were defined above by UV−vis spectroscopy, with the conformational states MI and MII, as defined by infrared spectroscopy. At pH 7.5 and 1 °C, we observe a pure MI state, which corresponds to the red-

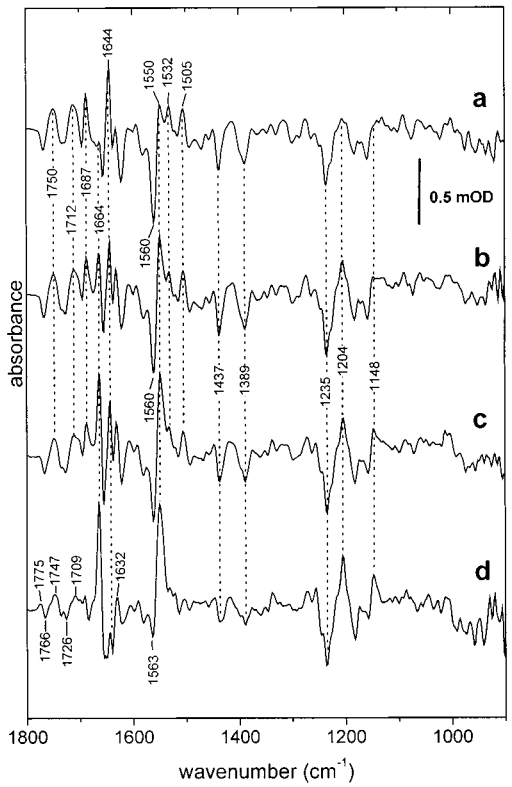

FIGURE 2: Infrared difference spectra of 9dm-Rho and its photoproducts in detergent (photoproduct minus dark state). The spectra were recorded from sandwich samples at 10 °C and pH 4.5 (spectrum a) and at 1 °C and pH 3.5 (spectrum b), pH 4.5 (spectrum c), and pH 7.5 (spectrum d).

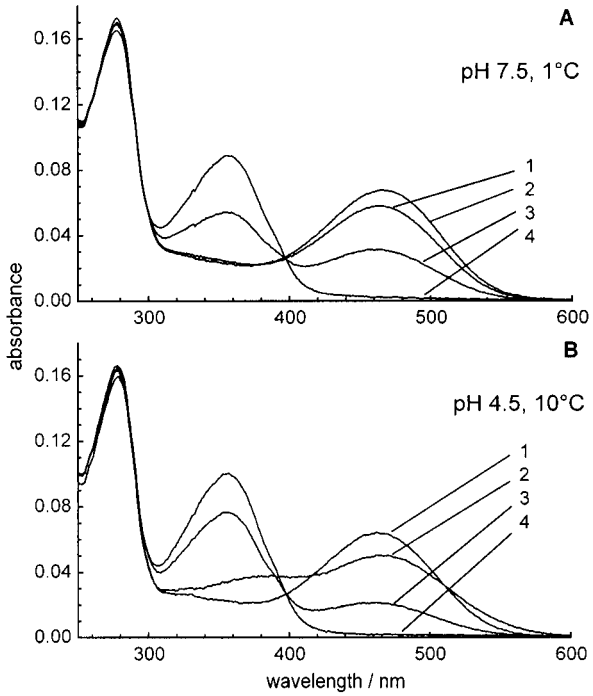

FIGURE 3: Determination of the extent of photoconversion and of the absorption coefficients of the photoproducts of 9dm-Rho. 9dm-Rho in detergent (trace 1: dark state) was illuminated for 1 min (trace 2) in 100 mM phosphate buffer, pH 7.5 and 1 °C (panel A), or pH 4.5 and 10 °C (panel B). After subsequent addition of 20 mM hydroxylamine, the samples were warmed to 25 °C, and the bleaching process was followed spectrophotometrically for approximately 1 h until no further spectral changes could be observed (trace 3). The samples were then entirely bleached with white light for 5 min (trace 4).

shifted photoproduct PP_{470}, that is observed under these conditions. On the other hand, the MII state observed at pH 4.5 and 10 °C is represented by both photoproducts PP_{380} and PP_{470}. MII consists therefore of two subspecies, MII_{380} and MII_{470}, with a deprotonated and a protonated Schiff base, respectively. Under conditions that allow formation of both MI and MII, PP_{470} may therefore be composed of a mixture of the spectrally almost degenerate MI and MII_{470} states, while PP_{380} always represents the MII_{380} subspecies (unless hydrolysis of the Schiff base has taken place).

9dm-Rho shows due to the similar λ_{max} of the dark state and PP_{470} considerable photoregeneration of the dark state. Under MI conditions (pH 7.5 and 1 °C) and illumination with wavelengths ≥475 nm only (45 ± 2)% (mean ± SD, Figure 3 A) of the pigment is converted into MI in the photostationary state. As extending the illumination time did not enhance photoproduct formation, the residual dark pigment is due to an equilibrium between photoproduct formation and photoregeneration of the dark state from the photoproducts. As we can measure the contribution of the dark state to the photoproduct spectra by the hydroxylamine method, we can also determine the true visible absorption maximum of MI to be at 470 nm with $\epsilon_{MI}/\epsilon_{dark} = 1.41 \pm 0.05$. The initial and the photoregenerated dark state are indistinguishable in respect to λ_{max} and ϵ, as assayed by bleaching of the two states in the presence of hydroxylamine and comparison of the resulting oxime peaks. They also show the same stability toward hydroxylamine and pH. We further determined λ_{max} of 9dm-Iso to be blue-shifted by 8 nm to 455 nm compared to 9dm-Rho in agreement with a previous study (*26*) with an absorption coefficient similar to that of 9dm-Rho. As λ_{max} of the initial and the photoregenerated dark states are indistinguishable, 9dm-Iso is not produced in appreciable amounts by photoregeneration from the MI state. This was further confirmed in FTIR spectra of 9dm-Iso. 9dm-Iso spectra are quite similar to 9dm-Rho spectra with major differences only in the fingerprint region with a strong negative band at 1209 cm^{-1}, which is not detected as a positive band in the photoproduct spectra of 9dm-Rho.

Under MII conditions (pH 4.5, 10 °C), the photoproduct yield is enhanced due to the formation of MII_{380}. (70 ± 2)% of the pigment is converted into MII_{380} and MII_{470} (Figure 3B). If we assume that the two MII subspecies have similar absorption coefficients, we can calculate $[MII_{380}]/([MII_{380}] + [MII_{470}])$, i.e., the portion of the MII photoproduct with a deprotonated Schiff base, to be 0.36 ± 0.01 (see Materials and Methods). This value seems to be constant for the solubilized pigment solutions under varying conditions, except for pH below 4.5, where the protonation equilibrium is shifted to the MII_{470} side. It also agrees with FTIR and UV−vis results from both detergent and membrane sandwich samples. For pH ≥4.5, ΔA_{380} can therefore be used to estimate the total MII content in a sample (see Materials and Methods). At pH 4.5 and 1 °C, we estimate from UV−vis spectra of pigment solutions, that the MI/MII photoproduct equilibrium is shifted to ~80% MII (Figure 1B), while UV−vis spectra from the corresponding sandwich samples indicate only approximately 50% MII (not shown), in agreement with FTIR spectra from the same samples. At 10 °C, spectra from both sample types agree with a largely MII photoproduct (Figure 1D,K), in line with FTIR spectra

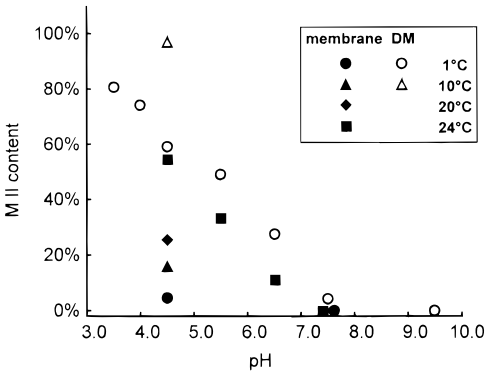

FIGURE 4: MII content in the MI/MII equilibrium of the photoproduct of 9dm-Rho in DM as assayed by infrared difference spectroscopy on sandwich samples in detergent (DM, open symbols) and membranes (closed symbols) at different temperatures (○, ●: 1 °C; △, ▲: 10 °C; ◆: 20 °C; ■: 24 °C).

(Figure 2a). This shows that the formation of MII may be reduced in sandwich samples compared to solutions, particularly at low temperatures, which may be due to the extremely high protein and detergent concentrations compared to solutions, which may interfere with MII formation.

As evident from the FTIR difference spectrum at 1 °C and pH 4.5 (Figure 2c), light-induced difference spectra of 9dm-Rho do in general not correspond to pure MI or MII difference spectra, but are rather described by linear combinations of these. For a quantification of the MII contents in the photoproduct, we used characteristic MII difference bands of Asp^{83}, Glu^{122}, and Glu^{113}, as described under Materials and Methods. With this method, we could examine the MI/MII equilibrium in 9dm-Rho systematically by infrared spectroscopy. The results of this investigation are summarized in Figure 4, where we show the MII content of the photoproduct of 9dm-Rho in dependence of pH, temperature, and environment of the pigment (detergent or membrane) in sandwich samples.

In membranes, no pure MII state could be obtained under the given experimental conditions (100 mM phosphate buffer) even at room temperature, but only under high ionic strength conditions, as will be described below. The MII content of the photoproduct increases therefore even at 24 °C from almost zero at pH 7.5 to only 55% at pH 4.5. At lower temperatures, MI prevails even more, and the mixture contains at pH 4.5 84% MI at 10 °C and 94% MI at 1 °C. It is not reasonable to extend experiments beyond 24 °C and below pH 4.5, as we observe under these conditions a massive hydrolysis of the photoproduct. This is evident from an overall decrease of difference bands in the protein range from 1800 to 1500 cm^{-1}, a decrease of the ethylenic mode of the chromophore at 1550 cm^{-1} and an overall change of the protein bands, particularly the amide bands. This resembles a partial refolding of the pigment to the dark state as observed before already for the decay of MII of Rho (*35*). As with detergent samples, the FTIR results on MII formation in membrane samples could be confirmed qualitatively by UV−vis spectra recorded from sandwich samples with pigment in membranes (Figure 1L,M). Due to the still considerable light scattering of the membrane films and the presence of retinal oxime and free retinal from the regeneration procedure, MII_{380} formation becomes evident only in the difference spectra (see insets in Figure 1L,M).

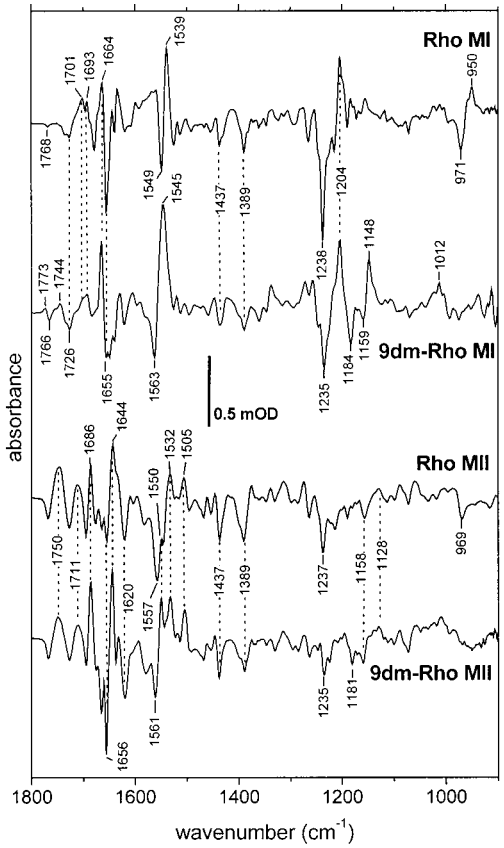

FIGURE 5: Infrared difference spectra of 9dm-Rho and its photoproducts in membranes in comparison to Rho (photoproduct minus dark state). The upper two spectra represent the MI state of Rho and the corresponding state in 9dm-Rho; the lower two spectra show the respective MII states. The Rho spectra were recorded from disk membranes in a pH 8.5 film sample at −3 °C with low hydration (MI) and a pH 4.5 sandwich sample at 1 °C (MII).

In detergent, we observe as stated above at pH 4.5 and 10 °C already an essentially pure MII difference spectrum and at 1 °C still almost 60% MII (Figure 2a,c). This percentage decreases again with increasing pH, and at pH 7.5 we have a pure MI state at 1 °C (Figure 2d). We extended the experiments at 1 °C to pH values below 4.5, as Schiff base hydrolysis is absent at this temperature. Interestingly, the MII content further increased to 80% at pH 3.5 (Figure 2b), as judged from the protonated carboxyl or the amide I bands, while UV−vis measurements indicated a decrease of the MII_{380} photoproduct when decreasing the pH to 3.5 (Figure 1A,B). As chromophore related bands as the fingerprint bands at 1204 and 1148 cm^{-1} and the ethylenic stretch mode at 1550 cm^{-1} are sensitive to the protonation state of the Schiff base, the effect of an increased MII formation on these bands may be partly compensated by the re-protonation of the Schiff base at a pH below 4.5. We can therefore conclude, that the re-protonation of the Schiff base at low pH only shifts the MII_{380}/MII_{470} equilibrium toward the 470 nm species and does not induce the formation of an acid MI species.

Infrared Properties of the MI State. Despite several similarities, the 9dm-Rho difference spectra of the pure MI photoproduct in membranes and detergent show distinct differences to the respective spectra derived from Rho. In the case of MI in membranes (Figure 5, upper two spectra), the intense +950/−971 cm^{-1} difference band of Rho MI,

which is assigned to the hydrogen-out-of-plane vibrations (HOOP modes) of the chromophore and a marker band of the Rho MI state, is missing in 9dm-Rho. In the fingerprint region of the two pigments between 1050 and 1300 cm^{-1}, the 1238 cm^{-1} band of a mode consisting of the $C_{12}-C_{13}$ stretch and $C_{15}H$ and NH bending modes (*36*) of the chromophore in the dark state of Rho is downshifted by 3 wavenumbers in 9dm-Rho. Two additional bands at 1184 and 1159 cm^{-1} characterize the dark state of 9dm-Rho, and two prominent bands at 1148 and 1204 cm^{-1} the MI photoproduct. The latter two bands sensitively reflect the protonation state of the Schiff base, as already described under Materials and Methods. In the region between 1300 and 1500 cm^{-1}, only minor differences between Rho and 9dm-Rho are observed. In the amide II region, which also comprises the ethylenic stretch mode of the chromophore, the $-1549/+1539$ cm^{-1} pattern of Rho is upshifted to $-1563/+1546$ cm^{-1} in 9dm-Rho. In the region of the amide I and the C=N stretch mode of the Schiff base between 1600 and 1700 cm^{-1}, we observe in 9dm-Rho slight variations of the band pattern in Rho. Particularly, the 1644 cm^{-1} photoproduct band in Rho is considerably reduced in 9dm-Rho, as well as the 1655 cm^{-1} band of the dark state, part of which is assigned to the C=N stretching mode of the Schiff base in Rho (*36*). The two dark state bands at 1735 and 1726 cm^{-1} are present both in Rho and in 9dm-Rho, while the band structure around 1701 cm^{-1} is altered and the positive 1744 cm^{-1} band is new in 9dm-Rho. The negative 1768 cm^{-1} band in Rho represents the Asp^{83} C=O stretch frequency in the dark state (*34*) and is downshifted in MI to 1764 cm^{-1}, while it is upshifted in the 9dm-Rho MI state giving rise to a $-1773/+1766$ cm^{-1} difference band, similar to the situation in rhodopsin − lumirhodopsin difference spectra (*22*). 9dm-Rho MI difference spectra derived from detergent samples (Figure 2d) correspond to those of membrane samples with some minor differences. For instance, the intense positive band at 1545 cm^{-1} in the amide II region is upshifted by 5 cm^{-1} in detergent, leading to a decreased intensity and also a slight upshift of the negative 1563 cm^{-1} band. The intensity of the positive amide I peak at 1664 cm^{-1} is slightly decreased and the band pattern in the carboxyl range shows some minor modifications, too.

Infrared Properties of the MII State. In contrast to the MI state of 9dm-Rho with its distinct differences to the corresponding Rho MI, the MII spectra of both pigments in membranes are very similar (Figure 5, lower two spectra). Particularly in the absorption range of protonated carboxyl groups above 1700 cm^{-1}, the spectra are not distinguishable. The equal intensities of the 1712 cm^{-1} photoproduct band in Rho and 9dm-Rho MII difference spectra imply that the counterion Glu^{113} becomes fully protonated in 9dm-Rho MII irrespective of the protonation state of the Schiff base. Major differences between Rho and 9dm-Rho MII are visible only in the amide II region, with a major photoproduct band at 1550 cm^{-1} in 9dm-Rho, which was previously assigned to the ethylenic stretch mode of the retinal chromophore with protonated Schiff base (*22*). This 1550 cm^{-1} band becomes weaker only for MII difference spectra recorded at 24 °C or higher temperatures and very acidic pH, which is due to the onset of hydrolysis of the retinal Schiff base and the release of free retinal, as described above. In detergent (Figure 2a), the spectra are only slightly changed, as, e.g., a negative band at 1733 cm^{-1} becomes visible, which is also observed in Rho MII difference spectra and which is due to removal of a difference band caused by lipids (*37*).

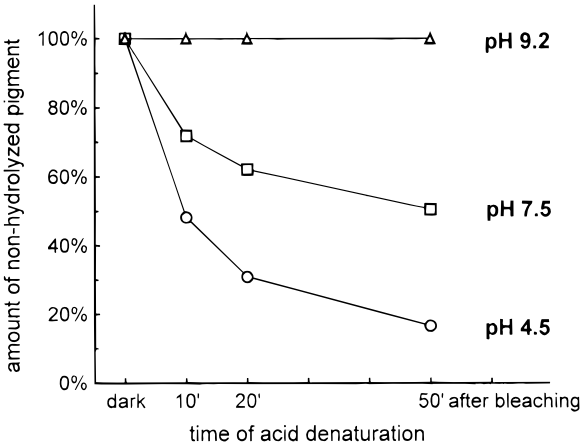

FIGURE 6: pH dependence of the Schiff base hydrolysis of the Rho MII photoproduct in detergent at 24 °C. The relative amount of pigment with a still intact Schiff base linkage was assayed by acid denaturation at the indicated time after complete bleaching of the samples at $t = 0$.

UV−Vis Results at Higher Temperatures and at Alkaline pH. At higher temperatures, we observe with detergent-solubilized 9dm-Rho also at pH 7.5 increasing amounts of the MII photoproduct as is evident from the PP_{380} contribution to the photoproduct spectrum at 10 and 24 °C (Figure 1E,H). At 24 °C, however, this MII formation is superimposed by a hydrolysis of the retinal Schiff base yielding free retinal and opsin, as shown by acid denaturation of the samples. Hydrolysis can be observed by UV−vis spectroscopy particularly at low pH and at temperatures above 10 °C. At 24 °C and pH 4.5 (Figure 1G), the 380 nm peak consists 20 min after illumination entirely of free retinal, as shown by acid denaturation, and the 470 nm peak shifts progressively with time to the blue side, which is interpreted as a slow denaturation of the protein. Particularly at room temperature, it is therefore necessary to distinguish carefully between MII_{380} and free retinal, which was already pointed out in a previous study (*28*). To assay whether this pH-dependence of Schiff base hydrolysis in the 9dm-Rho photoproducts reflects specific properties of its particular MII state or is merely acid catalyzed, we performed hydrolysis experiments with solubilized Rho in DM at 24 °C. In the assayed pH range from 4.5 to 9.2, solubilized Rho forms in contrast to 9dm-Rho only the MII photoproduct with a deprotonated Schiff base, which facilitates recognition of a direct pH effect. At different times after bleaching, samples were acid-denatured, and the amount of pigment with a still intact retinal Schiff base linkage was determined. Interestingly, no hydrolysis was observed at alkaline pH even 50 min after bleaching, while at pH 7.5 already 50% of the pigment was hydrolyzed to opsin and free retinal within that time (Figure 6). At pH 4.5, already 10 min after bleaching half of the pigment was hydrolyzed. This suggests that also in 9dm-Rho, the pH dependence of hydrolysis is at least partially due to the acid-catalyzed reaction mechanism. Indeed, at pH 8.5 and above, we observe no hydrolysis at either 10 or 24 °C (Figure 1F,J). Still a UV absorbing photoproduct can be observed, that rises at 1 and 10 °C

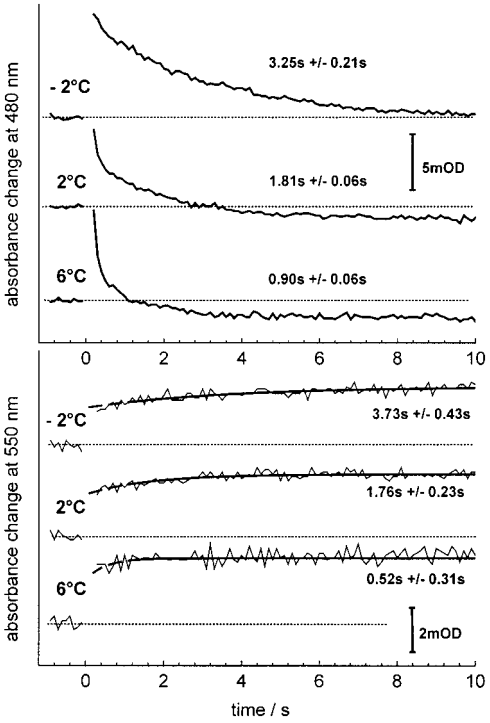

FIGURE 7: Kinetics of MII formation. Solubilized 9dm-Rho in 100 mM phosphate buffer, pH 4.5, was photolyzed at $t = 0$ at the indicated temperatures, and the subsequent absorbance changes were monitored at 480 nm for MII_{380} (A) and at 550 nm for MII_{470} (B). The stated values for the time constant τ were calculated from an exponential fit (mean ± SD from 3 experiments).

slowly and at 24 °C rapidly after illumination. As this 365 nm species can be titrated by diluted acid to a 430 nm species (data not shown), it is due to a progressive denaturation of the MI state of the protein under alkaline conditions. Infrared spectroscopy revealed that the 365 nm species appears in parallel with major changes of the initial MI spectrum being again indicative of a denaturation of the protein. As mentioned above, however, the retinal Schiff base linkage is not hydrolyzed under these conditions for at least 1 h.

Flash Photolysis of 9dm-Rho. To determine the apparent time constants of MII formation in 9dm-Rho, we carried out flash photolysis experiments at different temperatures in 100 mM phosphate buffer at pH 4.5, conditions that favor MII formation. Absorbance changes after photolysis of 9dm-Rho in DM were first recorded at 480 nm, where the difference spectrum between MI and the dark state reaches its maximum in order to measure the formation of MI and its subsequent decay to MII_{380}. At this wavelength we observe a rapid, unresolved absorbance increase after the flash due to MI formation, and a subsequent slower decay of the signal due to conversion to MII and partial deprotonation of the Schiff base (Figure 7 upper panel). Time constants of Schiff base deprotonation and thus formation of MII_{380} were determined by an exponential fit and are 3.2 s at −2 °C, 1.8 s at 2 °C, and 0.9 s at 6 °C. With Rho in detergent under same conditions, the kinetics of MII formation could not be resolved. A determination of the rate constants of MII_{470} formation was possible, because the visible absorption peaks of MI and MII_{470}, despite having similar λ_{max}, differ slightly in their bandwidth (see Figure 3). As the MII_{470} peak extends more to longer wavelengths compared to the MI peak, we can resolve MII_{470} formation selectively by monitoring absorbance changes at 550 nm. Again at this wavelength, we observe a rapid MI formation, which is followed by a slower increase due to conversion of MI to the MII_{470} species. The apparent time constants for the MI → MII_{470} transition are 3.7 s at −2 °C, 1.8 s at 2 °C, and around 0.5 s at 6 °C, in agreement with the time constants for MII_{380} formation.

Effect of Anions on the Spectral Properties of 9dm-Rho. Rhodopsin counterion mutants, that have Glu^{113} replaced by neutral residues were shown to possess different spectral properties due to a changed protonation state of the retinal Schiff base compared to Rho (*38*). In detail, the protonation state of the Schiff base in the dark pigment E113Q was shown to be directly related to the external pH, leading to a 380 nm species with an uncharged Schiff base at neutral to alkaline pH and a 490 nm species with a protonated Schiff base only at acidic pH. It could further be shown, that the Schiff base of the 380 nm species re-protonated after addition of halides and various other salts to the external medium and led to the formation of pigments absorbing in the visible range with the λ_{max} determined by the type of the anion serving as artificial counterion (*39, 40*).

As the MII state of 9dm-Rho possesses a (partially) protonated Schiff base despite of neutralization of Glu^{113}, the proposition is obvious that an anion may be recruited from the solvent in order to substitute for Glu^{113} as a new counterion to the protonated Schiff base in the MII_{470} state. To address this possibility, we examined the influence of isotonic amounts (150 mM) of various anions on the spectral properties of the photoproducts, particularly a possible shift of the MII_{380}/MII_{470} equilibrium to the MII_{470} side and an anion-dependent wavelength shift of the MII_{470} species. To be able to work in a well-buffered system, all experiments were performed in 100 mM MES buffer which has a comparatively bulky anion and proved to have no concentration-dependent influence on the spectral properties. As supplemented anions, we examined acetate, fluoride, chloride, bromide, iodide, and phosphate. We observed under mild conditions (pH 5.5, 1 °C) no anion specific shift of λ_{max}, but only a general salt-dependent slight increase in MII_{380} formation, which was also detected as an MII increase by FTIR spectroscopy. Iodide led to a more pronounced increase of the MII_{380} yield and was accompanied by a slow blue shift of the visible absorption maximum indicating destabilization and subsequent denaturation of the photoproduct. Under more acidic conditions (pH 4.0, 1 °C), we observed generally a slow denaturation of the 470 nm photoproduct, leading to a slow blue shift of its λ_{max} toward 430 nm, which was accelerated in the presence of halides, particularly with iodide.

The salt-dependent increase of the MII yield both depended on the ionic strength of the solvent and on the anion species. It was observed both by UV−vis and by FTIR spectroscopy in both detergent and membrane and will be described in detail elsewhere (Vogel, R., and Siebert, F., unpublished results). Possibly related effects were reported before on native Rho (*41, 42*). In a previous study on 9dm-Rho (*22*), the shifted MI/MII equilibrium of 9dm-Rho was not noticed due the inherent high ionic strength of film samples (>1 M phosphate) used for FTIR spectroscopy. Thus, the MII photoproduct observed by FTIR spectroscopy in high ionic strength pigment films was erroneously identified with the 470 nm peak seen by UV−vis spectros-

copy in low ionic strength pigment solutions, which only supported formation of MI.

DISCUSSION

In this paper, we studied the influence of the 9-methyl group of the retinal chromophore on the light-induced reaction cascade of rhodopsin leading to the active receptor state MII. For that purpose, we examined the properties of the artificial pigment 9dm-Rho consisting of the rhodopsin protein moiety opsin regenerated with the synthetic chromophore 11-cis 9-demethyl-retinal. This pigment shows several interesting properties which distinguish it from native rhodopsin in several respects and may help to elucidate the role of the 9-methyl group in the activation process of rhodopsin.

9dm-Rho Shows a Shifted MI/MII Equilibrium. In 9dm-Rho, the equilibrium between the physiologically important late intermediates MI and MII of the receptor activation cascade is dramatically shifted to the MI side, the immediate precursor of the active receptor state MII. This is apparent both in its native membrane environment as well as in detergent micelles. Solubilized Rho forms full MII even at 0 °C and pH 8.5 (data not shown). 9dm-Rho forms under otherwise the same conditions no MII. Moreover, the kinetics of receptor activation are slowed by 2 orders of magnitude. While in solubilized Rho MII is formed with a time constant of 10 ms (*43*), in 9dm-Rho the same reaction takes place on the time range of seconds.

In membranes, Rho has a pH-dependent MI/MII equilibrium which is due to protonation changes of Glu^{134} on helix 3 at the cytoplasmic interface and presumably also other groups (*44*). In detergent micelles with flexible alkyl chains, the barrier for MII formation is lowered and no longer depends on proton uptake, which occurs in a separate subsequent reaction at low pH (*43*). In 9dm-Rho, protonation is still required for MII formation even in detergent micelles, rendering the MI/MII equilibrium also for solubilized pigment sensitive to pH. Even as compared to Rho in its native membrane environment (*45*), 9dm-Rho in DM has both a lower MII/MI ratio and a lower observed rate constant for MII formation. MII formation of 9dm-Rho depends moreover sensitively on the water content of the matrix it is embedded in. A reduced water content in pigment films severely hampers MII formation, rendering 9dm-Rho much more sensitive to the water content of film samples than Rho. This effect over-compensates the reported enhanced Rho MII formation upon osmotic binding of water (*42*).

From the kinetics of MII formation, it is obvious that the presence of the 9-methyl group of the retinal in Rho decreases the activation free energy $\Delta G^{\#}$ of the MI to MII transition compared to 9dm-Rho. The impact of the 9-methyl group on the MI/MII equilibrium consists similarly in a decrease of the standard free energy change ΔG_0 between MI and MII. ΔG_0 is considerably less negative (or more positive) in the case of 9dm-Rho as compared to Rho, as is evident from the drastic shift of the equilibrium constants. Preliminary evaluation of the MI/MII equilibrium of 9dm-Rho in membranes suggests that this change in ΔG_0 is rather due to a decrease in ΔS_0 than an increase in ΔH_0. Arrhenius fits to our data at pH 4.5 and in the temperature range from 1 to 24 °C are in agreement with a ΔH_0 of (79 ± 9) kJ/mol as reported before for native Rho in disk membranes (*45*), while ΔS_0 is concomitantly decreased.

To clarify the molecular background of these changes in 9dm-Rho, it is helpful to recall first the situation in native Rho. In Rho, the MI to MII transition can be considered to be a transition between a state (MI), which is governed by a thermodynamically optimized conformation of the chromophore and its immediate protein environment (i.e., its binding pocket), and a more flexible state (MII), in which the protein on the whole is in a thermodynamic minimum (*8*). Chromophore−protein interactions should thus be structurally important particularly in the MI state. We therefore propose that the steric interaction between the retinal 9-methyl group and specific residues on helices 3 and 6 in native Rho consists largely in a restriction of the conformational space accessible to the MI state. Removal of this interaction in the 9dm-Rho pigment relieves this restriction, and therefore allows MI more conformational freedom for the chromophore and probably also the protein moiety in this modified pigment. In thermodynamic parameters, removal of this interaction in 9dm-Rho leads to an increase of the entropy of the MI state in this pigment compared to Rho. This increase in entropy may already be present in the states preceding MI formation including the dark pigment. If we consider the entropy of the MII state to be rather unaffected by the steric interaction, which is in line with the picture described above, the entropy gain of the transition to MII should be lowered in 9dm-Rho. This in turn renders the standard free energy change ΔG_0 of the MI/MII transition less negative (or more positive, depending on position of the equilibrium), and thus shifts the corresponding equilibrium to the MI side. The increased ΔG_0 may in part also be responsible for the increased $\Delta G^{\#}$ of the MI to MII transition in 9dm-Rho. With these changes in the thermodynamic parameters for 9dm-Rho, MII should be formed only at higher temperatures. Moreover, the influence of parameters that change the enthalpy term of ΔG_0 by a similar absolute amount in both Rho and 9dm-Rho should be more sensitively reflected in 9dm-Rho due to the decreased counteracting entropy term. Such a parameter may for instance be the fluidity of the environment in which the pigment is embedded.

The Dark State. The dark state of 9dm-Rho is distinguished from the Rho dark state by the λ_{max} blue-shifted by 36 nm to 464 nm compared to the only 7 nm difference of the respective free retinals. As described above, we also derived a reduced extinction coefficient for dark 9dm-Rho. Both observations hint to a conformation of the chromophore in its binding pocket which significantly differs from that in Rho. The blue-shifted absorption maximum is possibly due to a stronger interaction of the counterion with the Schiff base. In the case of Rho, NMR investigations have placed the counterion close to $C_{12}-C_{13}$, i.e., rather far away from the Schiff base (*46*). Thus, removal of the 9-methyl group could bring the Schiff base closer to the counterion Glu^{113}, thereby inducing the blue-shift. The observation of an almost identical C=N stretch mode in Rho and 9dm-Rho (*22*) is not in contradiction, since it has been shown that its frequency does not reflect the electrostatic interaction but is mainly determined by hydrogen bonding (*47*).

A changed conformation of the chromophore in its binding pocket is also inferred by the lack of the intense Rho 967

cm^{-1} HOOP band of the 11−12-hydrogen-out-of-plane bending mode, which is due to a twisted chromophore structure in Rho, and a change of the band pattern in the fingerprint region, particularly a 3 cm^{-1} downshift and reduction of the 1238 cm^{-1} mode, which sensitively reflects chromophore−protein interactions in the neighborhood of the Schiff base up to the C_{12} of the chromophore (*36*). The chromophore fits therefore presumably more relaxed in its binding pocket in the dark state, a proposal which is also supported by infrared spectroscopy of its immediate photoactivation intermediates bathorhodopsin and lumirhodopsin (*22*). In the range from 900 to 1300 cm^{-1}, covering both fingerprint and HOOP region, the difference spectra of both 9dm-Rho intermediates are already very similar to our MI spectra, in contrast to the corresponding Rho intermediates. This is in line with the proposed higher entropy of the dark state in 9dm-Rho compared to Rho. The positions of the C═O stretch mode of the protonated carboxyl groups of Asp^{83} and Glu^{122} are unchanged in dark 9dm-Rho and may together with the unchanged stability of the dark pigment toward hydroxylamine hint to a rather similar protein conformation in both dark pigments.

The MI State. Transition to the MI state is accompanied by a slight 6 nm red-shift of the visible absorption maximum to 470 nm, together with a 1.4-fold increase of the absorption coefficient. Infrared difference spectra reveal major differences between the MI states of Rho and 9dm-Rho, as is evident in the range from 1500 to 1700 cm^{-1}. These differences may indicate that the transitions comprise different conformational changes, becoming evident in the amide I and II bands. In addition, they also reflect shifts in the frequencies of the C═N Schiff base stretch mode and of the delocalized C═C ethylenic stretch mode of the chromophore. While in lumirhodopsin and MI of Rho major changes of the Schiff base environment were observed by shifts of the C═N Schiff base stretch frequency (*48*), these are absent in the respective photoproducts of 9dm-Rho (*22*). The differences in the spectral range of protonated carboxyl groups between Rho and 9dm-Rho indicate diverging environments for both Asp^{83} and Glu^{122} in the two pigments, which may serve as markers for conformational changes in the protein. The upshift of the Asp^{83} frequency in 9dm-Rho MI reflects an slightly more hydrophobic environment of the carboxyl group in MI compared to the dark state. The same might apply for Glu^{122}, as the 1700 cm^{-1} MI band in Rho is reduced in 9dm-Rho and instead an upshifted 1744 cm^{-1} photoproduct band arises in membranes and even more pronounced in the micellar matrix of detergent solubilized Rho. Changes of the Glu^{122} carboxyl bands were also detected in rhodopsin − bathorhodopsin difference spectra upon mutation of Gly^{121} to alanine (*49*). Therefore, the altering of Glu^{122} bands in 9dm-Rho MI may also reflect local steric changes due to the lack of the 9-methyl group. Most interestingly in 9dm-Rho MI difference spectra, the intense HOOP bands are missing, which usually serve as marker bands for Rho MI. The infrared intensities of HOOP bands are related to twists in the chromophore structure, which store the energy of the absorbed photon in the early intermediates of the Rho reaction cascade (*19*). In resonance Raman spectra of Rho MI (*21*), the 956 cm^{-1} HOOP mode is shifted and much more intense compared to the respective mode in an all-trans protonated model Schiff base or MII. As the respective Rho MII spectrum corresponds to the spectrum of an all-trans unprotonated model Schiff base, we conclude that some of the chromophore distortions present in lumirhodopsin or bathorhodopsin still persist in Rho MI, while they are relieved in Rho MII. A lack of these HOOP bands in 9dm-Rho MI may therefore indicate a relaxed fit of the chromophore in the retinal binding pocket already in the MI state. This would be in agreement with the 9-methyl group of the retinal holding helix 3 and/or 6 "in position" in the corresponding Rho MI state. The 9dm-retinal would therefore allow the protein a higher degree of freedom in packing around the chromophore (but still far less than in the MII state). Vice versa, the 9dm-retinal may be less restricted than its methylated native counterpart in the same binding pocket, leading to a higher flexibility of the chromophore in 9dm-Rho compared to native Rho. Both models yield a higher entropy of the MI state in the absence of the 9-methyl group than in its presence. The results presented in this study suggest that both models apply: the 9dm-Rho MI state has a protein conformation different from Rho MI as evident from the carboxyl bands. In addition, already in 9dm-Rho bathorhodopsin and lumirhodopsin the chromophore related infrared difference bands are similar to 9dm-Rho MI (*22*) and indicate in all states a less strained and restricted chromophore. Thus the resulting entropy increase of the 9dm-Rho MI state appears to be the very reason for the dramatic shift of the MI/MII equilibrium in 9dm-Rho.

The Active Receptor State MII and Photoregeneration. Infrared difference spectra of Rho and 9dm-Rho are almost indistinguishable from their MII photoproduct bands. The only major difference is the 1550 cm^{-1} photoproduct band in 9dm-Rho, which was assigned previously to the ethylenic stretch mode of a chromophore with a still protonated Schiff base (*22*). This is reflected in the UV−vis spectra of the MII photoproduct, revealing two subspecies MII_{470} and MII_{380} with a protonated and deprotonated Schiff base, respectively, being in an apparently constant proportion of about 60:40. Only at low pH below 4.5, we observe in the UV−vis range a decrease of the MII_{380} species. This decrease is not due to the formation of a low pH MI species, but rather due to a shift in the MII_{380}/MII_{470} protonation equilibrium. Evidence for this comes from the long-wavelength tail of the 470 nm peak, which allows a distinction between MI and MII_{470}, and from the still increasing MII content at pH 3.5 derived from the FTIR data. The shift in the MII_{380}/MII_{470} protonation equilibrium is presumably facilitated by a destabilization of the protein at a pH below 4.5 and a concomitantly increased sensitivity of the Schiff base protonation state to the bulk pH.

The only partial Schiff base deprotonation in MII has major implications on experiments with 9dm-Rho. In Rho, the transition from MI to MII is strictly coupled to the transfer of the Schiff base proton to Glu^{113} (*12*), leading to a blue-shift of the MII photoproduct to 380 nm. This wavelength shift allows under appropriate illumination conditions complete conversion of the dark pigment into the MII photoproduct in Rho. Due to the almost perfect overlap of the visible absorption peaks of the dark, MI and MII_{470} state of 9dm-Rho, together with a drastically slowed transition to MII, we have considerable photoregeneration of the dark state upon illumination of the pigment, particularly

under conditions, where only little MII and therefore little MII_{380} is formed. Even with an optimized wavelength selection the conversion yield will not reach 50% under MI conditions, as the MI extinction coefficient is increased compared to the dark state. When examining MI/MII equilibria, care has therefore to be taken to distinguish the three spectrally almost degenerate states, e.g., by the hydroxylamine method to assay the regenerated dark pigment and by extrapolation of the MII_{380} subspecies to the total MII content. Interestingly, only 9dm-Rho with the 11-cis chromophore is formed by photoregeneration and no 9dm-Iso with a 9-cis chromophore. The latter pigment has an absorption maximum which is blue-shifted by 8 nm compared to 9dm-Rho.

We can only speculate on the molecular cause for the presence of the two MII subspecies in 9dm-Rho. In Rho, Glu^{113}, which serves as the counterion to the protonated Schiff base in the dark state, is neutralized in MII by proton transfer from the Schiff base (*12*). This mechanism is modified in 9dm-Rho MII, as Glu^{113} becomes protonated irrespective of the residual 60% Schiff base protonation. The requirement of Glu^{113} neutralization for MII formation could therefore be further confirmed. It was argued before (*22*), that the charged Schiff base in MII might be stabilized by recruitment of an inorganic anion from the solvent phase serving as a new counterion to the protonated Schiff base in the MII_{470} subspecies. This picture could not be confirmed in this study, as supplementing the solvent with a variety of anions did not lead to detectable changes of the λ_{max} of the MII_{470} species nor to a shift of the MII Schiff base protonation equilibrium to the MII_{470} side. Such anion-dependent changes were observed with the dark state of site-directed mutants of Rho, where the counterion Glu^{113} was replaced by an uncharged residue (*39, 40*). Our data are consistent with a stabilization of the protonated Schiff base in the MII_{470} state by internal bound water molecules serving to shield the Schiff base proton in an environment with an otherwise low dielectric constant. This may involve a changed position of the Schiff base in 9dm-Rho MII compared to Rho MII. It was shown previously that in model compounds the pK_a of the Schiff base sensitively depends on the particular structure of hydrogen bonds to water molecules in the environment of the Schiff base (*50*).

Activity of the 9dm-Rho MII State. Previous studies addressed the ability of 9dm-Rho photoproducts to activate the visual G-protein transducin (*22, 28*) and the excitation and subsequent desensitization of salamander rod cells regenerated with 9dm-retinal (*29, 30*). The latter studies revealed a 30 times decreased quantal response upon flash illumination of the modified pigment and a subsequent 5-fold prolongation of the decay of the active state, as well as a maximal initial rate of phosphorylation of ROS 9dm-Rho being only 25% of the respective rate of native ROS pigment. These results agree well with the presented results on 9dm-Rho activation. Under the reported assay conditions (e.g., neutral pH), the MI/MII equilibrium in the 9dm-pigments is shifted to the MI side, such that initially only little MII is formed compared to the native pigments. Desensitization of the rod cells, which proceeds via MII-specific phosphorylation by rhodopsin kinase and subsequent binding of arrestin, will proceed only at a decreased rate. Moreover, desensitized MII is no longer in equilibrium with pigment in the MI state, such that new MII will be formed from the MI pool, thus leading to a reduced, but prolonged excitation of the rod cells.

Activation of the visual G-protein transducin by MII can be assayed by different methods, e.g., by detecting changes of the intrinsic transducin α-subunit $G_{t\alpha}$ fluorescence upon nucleotide exchange (*51*) or by a filter binding assay for $G_{t\alpha}$ with bound, radioactively labeled GTP-γ-S (*52*). The first method involves irradiation of the dark pigment with UV-light, which leads to excitation of tryptophan side chains in the retinal binding pocket of the pigment and besides fluorescence also to energy transfer to the neighboring bound retinal. Considering the complicated bleaching behavior, this would lead to shifts in the photoproduct yields, which are difficult to control and render a quantitative comparison between transducin activation and the amounts of the single photoproducts impossible. We therefore rather tried to correlate published studies based on filter binding assays (*22, 28*) with the results presented in this paper.

The most recent study on transducin activation by solubilized 9dm-Rho revealed 37% activity compared to opsin regenerated with 11-*cis*-retinal at 25 °C, pH 7.2, and continuous illumination with light above 495 nm (*28*). To analyze MII activity, we determined MII formation ($MII_{380} + MII_{470}$) by UV−vis spectroscopy under comparable conditions to be only about 33% of the total pigment. This low MII yield is not only due to the shifted MI/MII equilibrium, but also due to considerable photoregeneration of the dark state, which is favored under long-wavelength illumination. The contribution of the 380 nm species to the photoproduct is only about 12% of the total pigment, in accordance with the original spectra (*28*).

There was further disagreement with another transducin activation study (*22*) that reported only 9% and 27% activity under illumination with orange (cutoff 540 nm) and white light, respectively (values corrected for regeneration efficiency with 11-*cis*-retinal). Pigment was illuminated at 4 °C and then transferred to the 20 °C assay buffer at pH 7.4 in the dark. Under these conditions, we determined the initial conversion to be 50% with white light, and the MII content of the photoproduct to be about 50% under final assay conditions, yielding a total of only 25% MII, in agreement with the transducin activation results. Upon illumination with orange light, the photoproduct yield will again be severely decreased and thus lead to the observed low activity levels.

These results show that the activity of the 9dm-Rho pigment directly corresponds to the amount of MII (consisting of *both* subspecies MII_{380} and MII_{470}) being formed with a relative activity comparable to that of native Rho MII. If only the 380 nm species were in the active state, a more than 3-fold activity of this species would be required compared to that of Rho MII, which seems very unlikely. We can therefore conclude that in the 9dm-Rho photoproducts presumably both MII_{380} and MII_{470} activate transducin, regardless of the protonation state of the Schiff base. This is in full agreement with the infrared difference spectra, that indicate besides the 1550 cm^{-1} band marking the only partially deprotonated Schiff base no major differences between the MII states of both Rho and 9dm-Rho. Schiff base deprotonation, the signature for Rho MII (*6*), is in the case of 9dm-Rho not a prerequisite for formation of the active receptor. The significance of the retinal 9-methyl group is therefore not based on a particular influence on properties

of the active MII conformation itself, as this conformation is functionally not changed in 9dm-Rho. It must rather be seen in its impact on the precursors of and the transition to MII, which is slowed by 2 orders of magnitude in its absence, and the shifted equilibrium. The steric constraints imposed by the 9-methyl group onto the Rho MI state can be clearly resolved by infrared spectroscopy, as well as the release of these constraints in the corresponding 9dm-Rho state. The concomitant entropy increase of this state finally leads to the observed dramatic shift of the MI/MII equilibrium in 9dm-Rho, rendering the retinal 9-methyl group a crucial determinant of rhodopsin activation.

Future Questions. 9dm-Rho differs from Rho not only in the changed MI/MII equilibrium, but also in the broad shape of the pH dependence of its activation. From previous studies on Rho activation, it is known that MII formation is coupled to proton uptake (*13*, *43*, *45*, *53*). One can distinguish between protons being essential and nonessential for the transition itself (*4*, *45*). Due to the Schiff base protonation equilibrium, formation of 9dm-Rho MII should require 0.6 proton for the protonation of Glu^{113} in addition to the 0.7−1.0 essential proton required by Rho (*13*, *45*, *53*). As this additional 0.6 proton is again rather essential for the transition, we expect a complicated interplay between the two different pK_a values, which may in turn lead to the broad pH profile observed for MII formation in 9dm-Rho. Studies to investigate the proton uptake by 9dm-Rho and to resolve these questions are in progress.

NOTE ADDED IN PROOF

During the reviewing process of this article a paper on properties of COS-expressed solubilized 9dm-Rho appeared (*54*). While the authors arrive at similar conclusions regarding the MI/MII equilibrium of 9dm-Rho, the properties of the MII photoproduct of their pigment seem to be different.

ACKNOWLEDGMENT

We thank B. Mayer for technical assistance in the protein preparation, K. Fahmy and J. Isele for helpful discussion, and T. Sakmar for critically reading the manuscript.

REFERENCES

1. Sakmar, T. P. (1998) *Prog. Nucleic Acid Res. Mol. Biol 50*, 1−34.
2. Peteanu, L. A., Schoenlein, R. W., Wang, Q., Mathies, R. A., and Shank, C. V. (1993) *Proc. Natl. Acad. Sci. U.S.A. 90*, 11762−11766.
3. Shichida, Y. (1986) *Photobiochem. Photobiophys. 13*, 287−307.
4. Hofmann, K. P. (1986) *Photobiochem. Photobiophys. 13*, 309−327.
5. Emeis, D., Kühn, H., Reichert, J., and Hofmann, K. P. (1982) *FEBS Lett. 143*, 29−34.
6. Longstaff, C., Calhoon, R. D., and Rando, R. R. (1986) *Proc. Natl. Acad. Sci. U.S.A. 83*, 4209−4213.
7. Cooper, A. (1981) *FEBS Lett. 123*, 324−326.
8. Shichida, Y. and Imai, H. (1998) *Cell. Mol. Life Sci. 54*, 1299−1315.
9. Farahbakhsh, Z. T., Hideg, K., and Hubbell, W. L. (1993) *Science 262*, 1416−1419.
10. Sheikh, S. P., Zvyaga, T. A., Lichtarge, O., Sakmar, T. P., and Bourne, H. R. (1996) *Nature 383*, 347−350.
11. Farrens, D. L., Altenbach, C., Yang, K., Hubbell, W. L., and Khorana, H. G. (1996) *Science 274*, 768−770.
12. Jäger, F., Fahmy, K., Sakmar, T. P., and Siebert, F. (1994) *Biochemistry 33*, 10878−10882.
13. Arnis, S., Fahmy, K., Hofmann, K. P., and Sakmar, T. P. (1994) *J. Biol. Chem. 269*, 23879−23881.
14. Han, M., Groesbeek, M., Sakmar, T. P., and Smith, S. O. (1997) *Proc. Natl. Acad. Sci. U.S.A. 94*, 13442−13447.
15. Shieh, T., Han, M., Sakmar, T. P., and Smith, S. O. (1997) *J. Mol. Biol. 269*, 373−384.
16. Han, M., Lin, S. W., Minkova, M., Smith, S. O., and Sakmar, T. P. (1996) *J. Biol. Chem. 271*, 32337−32342.
17. Pogozheva, I. D., Lomize, A. L., and Mosberg, H. I. (1997) *Biophys. J. 72*, 1963−1985.
18. Herzyk, P. and Hubbard, R. E. (1998) *J. Mol. Biol. 281*, 741−754.
19. Palings, I., van den Berg, E. M., Lugtenburg, J., and Mathies, R. A. (1989) *Biochemistry 28*, 1498−1507.
20. Bagley, K. A., Balogh-Nair, V., Croteau, A. A., Dollinger, G., Ebrey, T. G., Eisenstein, L., Hong, M. K., Nakanishi, K., and Vittitow, J. (1985) *Biochemistry 24*, 6055−6071.
21. Doukas, A. G., Aton, B., Callender, R. H., and Ebrey, T. G. (1978) *Biochemistry 17*, 2430−2435.
22. Ganter, U. M., Schmid, E. D., Perez-Sala, D., Rando, R. R., and Siebert, F. (1989) *Biochemistry 28*, 5954−5962.
23. Han, M., Lin, S. W., Smith, S. O., and Sakmar, T. P. (1996) *J. Biol. Chem. 271*, 32330−32336.
24. Han, M., Lou, J., Nakanishi, K., Sakmar, T. P., and Smith, S. O. (1997) *J. Biol. Chem. 272*, 23081−23085.
25. Blatz, P. E., Lin, M., Balasubramaniyan, P., Balasubramaniyan, V., and Dewhurst, P. B. (1969) *J. Am. Chem. Soc. 91*, 5930−5931.
26. Kropf, A., Whittenberger, B. P., Goff, S. P., and Waggoner, A. S. (1973) *Exp. Eye Res. 17*, 591−606.
27. Randall, C. E., Lewis, J. W., Hug, S. J., Björling, S. C., Eisner-Stans, I., Friedman, N., Ottolengi, M., Sheves, M., and Kliger, D. S. (1991) *J. Am. Chem. Soc. 113*, 3473−3485.
28. Han, M., Groesbeek, M., Smith, S. O., and Sakmar, T. P. (1998) *Biochemistry 37*, 538−545.
29. Morrison, D. F., Ting, T. D., Vallury, V., Ho, Y. K., Crouch, R. K., Corson, D. W., Mangini, N. J., and Pepperberg, D. R. (1995) *J. Biol. Chem. 270*, 6718−6721.
30. Corson, D. W., Cornwall, M. C., MacNichol, E. F., Tsang, S., Derguini, F., Crouch, R. K., and Nakanishi, K. (1994) *Proc. Natl. Acad. Sci. U.S.A. 91*, 6958−6962.
31. Kahlert, M., König, B., and Hofmann, K. P. (1990) *J. Biol. Chem. 265*, 18928−18932.
32. DeGrip, W. J. (1982) *Methods Enzymol. 81*, 197−207.
33. Waddel, W., Umerua, M., and West, J. (1978) *Tetrahedron Lett. 35*, 3223−3226.
34. Fahmy, K., Jäger, F., Beck, M., Zvyaga, T. A., Sakmar, T. P., and Siebert, F. (1993) *Proc. Natl. Acad. Sci. U.S.A. 90*, 10206−10210.
35. Rothschild, K. J., Gillespie, J., and DeGrip, W. J. (1987) *Biophys. J. 51*, 345−350.
36. Siebert, F. (1995) *Isr. J. Chem. 35*, 309−323.
37. Beck, M., Siebert, F., and Sakmar, T. P. (1998) *FEBS Lett. 436*, 304−308.
38. Sakmar, T. P., Franke, R. R., and Khorana, H. G. (1989) *Proc. Natl. Acad. Sci. U.S.A. 86*, 8309−8313.
39. Nathans, J. (1990) *Biochemistry 29*, 9746−9752.
40. Sakmar, T. P., Franke, R. R., and Khorana, H. G. (1991) *Proc. Natl. Acad. Sci. U.S.A. 88*, 3079−3083.
41. Delange, F., Merkx, M., Bovee-Geurts, P. H., Pistorius, A. M., and DeGrip, W. J. (1997) *Eur. J. Biochem. 243*, 174−180.
42. Mitchell, D. C. and Litman, B. J. (1999) *Biochemistry 38*, 7617−7623.
43. Arnis, S. and Hofmann, K. P. (1993) *Proc. Natl. Acad. Sci. U.S.A. 90*, 7849−7853.
44. Fahmy, K. and Sakmar, T. P. (1993) *Biochemistry 32*, 7229−7236.
45. Parkes, J. H. and Liebman, P. A. (1984) *Biochemistry 23*, 5054−5061.

46. Han, M., DeDecker, B. S., and Smith, S. O. (1993) *Biophys. J. 65*, 899−906.
47. Livnah, N. and Sheves, M. (1993) *J. Am. Chem. Soc. 115*, 351−353.
48. Ganter, U. M., Gärtner, W., and Siebert, F. (1988) *Biochemistry 27*, 7480−7488.
49. Nagata, T., Terakita, A., Kandori, H., Shichida, Y., and Maeda, A. (1998) *Biochemistry 37*, 17216−17222.
50. Gat, Y. and Sheves, M. (1993) *J. Am. Chem. Soc. 115*, 3772−3773.
51. Phillips, W. J. and Cerione, R. A. (1988) *J. Biol. Chem. 263*, 15498−15505.
52. Wessling-Resnick, M. and Johnson, G. L. (1987) *J. Biol. Chem. 262*, 3697−3705.
53. Bennett, N. (1980) *Eur. J. Biochem. 111*, 99−103.
54. Meyer, C. K., Böhme, M., Ockenfels, A., Gärtner, W., Hofmann, K. P., and Ernst, O. P. (2000) *J. Biol. Chem. 275*, 19713−19718.

BI000852B